

SPECTROGRAPHIC STUDY OF THE SEYFERT GALAXY NGC 3227*

VERA C. RUBIN AND W. KENT FORD, JR.

Department of Terrestrial Magnetism, Carnegie Institution of Washington, Washington, D.C.,
and Kitt Peak National Observatory,† Tucson, Arizona*Received March 18, 1968; revised May 20, 1968*

ABSTRACT

Image-tube spectra of the Seyfert galaxy NGC 3227 have been obtained at a dispersion of 132 \AA mm^{-1} , centered near $H\alpha$. Broad emission lines of $H\alpha$, $H\beta$, $[\text{O III}] \lambda\lambda 4959, 5007$, $[\text{O I}] \lambda\lambda 6300, 6364$, $[\text{N II}] \lambda\lambda 6548, 6583$ are observed; a G-type absorption-line spectrum is also present. Measured velocities of the broad emission lines in the nuclear region ($r < 200 \text{ pc}$) indicate that discrete gas clouds are moving with velocities which range over several thousand kilometers per second. These clouds have a mean negative velocity with respect to the central velocity due to the motions of clouds expanding from the nucleus. Line strengths are determined, and mean values of T and N_e calculated.

In the disk of NGC 3227, sharp lines of $H\alpha$ and $[\text{N II}]$ are observed, which give a linear rotation curve out to $r = 600 \text{ pc}$. Emission is also observed at $r = 3900 \text{ pc}$ and in the connecting arm between NGC 3227 and its elliptical companion, NGC 3226; this gas has a velocity of -700 km sec^{-1} with respect to the mean NGC 3226/3227 velocity. The spectrum of the elliptical companion NGC 3226 has emission lines of $H\alpha$, $[\text{N II}] \lambda\lambda 6548, 6583$, and $H\beta$.

I. INTRODUCTION

NGC 3227 is one of the galaxies originally listed by Seyfert (1943) because its spectrum shows broad, high-excitation emission lines superimposed upon a solar-like continuum. However, it was not observed by Seyfert, and it remains, together with NGC 5548, one of the two galaxies on his list for which recent spectrographic studies have not been made. NGC 3227 has a bright semistellar nucleus, surrounded by faint spiral structure containing patchy emission regions. The orientation of the plane of the galaxy to the line of sight is favorable for studying the rotation of the galaxy. Like several other Seyfert galaxies, NGC 3227 has a companion, the elliptical galaxy NGC 3226 (K?, E3, Morgan 1959), and long-exposure photographs indicate that the outer northwest arm of NGC 3227 connects with NGC 3226. On the *Palomar Sky Survey* prints, both NGC 3227 and NGC 3226 are overexposed, but very distant outer irregular structure is seen surrounding NGC 3227. Morgan (1959) has called attention to the resemblance of NGC 3226/3227 to NGC 5194/5195 (M51).

We show in Figure 1 (Plate 2) a direct plate of NGC 3227 and NGC 3226 taken with the 40-inch Richey-Chrétien telescope of the U.S. Naval Observatory in Flagstaff, Arizona, in which the semistellar nucleus of NGC 3227 is seen. In Figure 1 we also reproduce the image as it appears on the blue print of the *Palomar Sky Survey*. Although the nucleus of NGC 3227 is overexposed, the connecting arm between the two galaxies is visible. On the original *Palomar Sky Survey* print there is distant irregular structure which is off the field of the copy in Figure 1. A photograph of NGC 3226/3227 has also been published by Burbidge, Burbidge, and Sandage (1963).

II. OBSERVATIONS

Spectra of NGC 3227 and NGC 3226 have been obtained with the DTM spectrograph attached to the 72-inch Perkins telescope of Ohio State and Ohio Wesleyan Uni-

* *Contributions from the Kitt Peak National Observatory*, No. 338.

† Operated by the Association of Universities for Research in Astronomy, Inc., under contract with the National Science Foundation.

PLATE 2

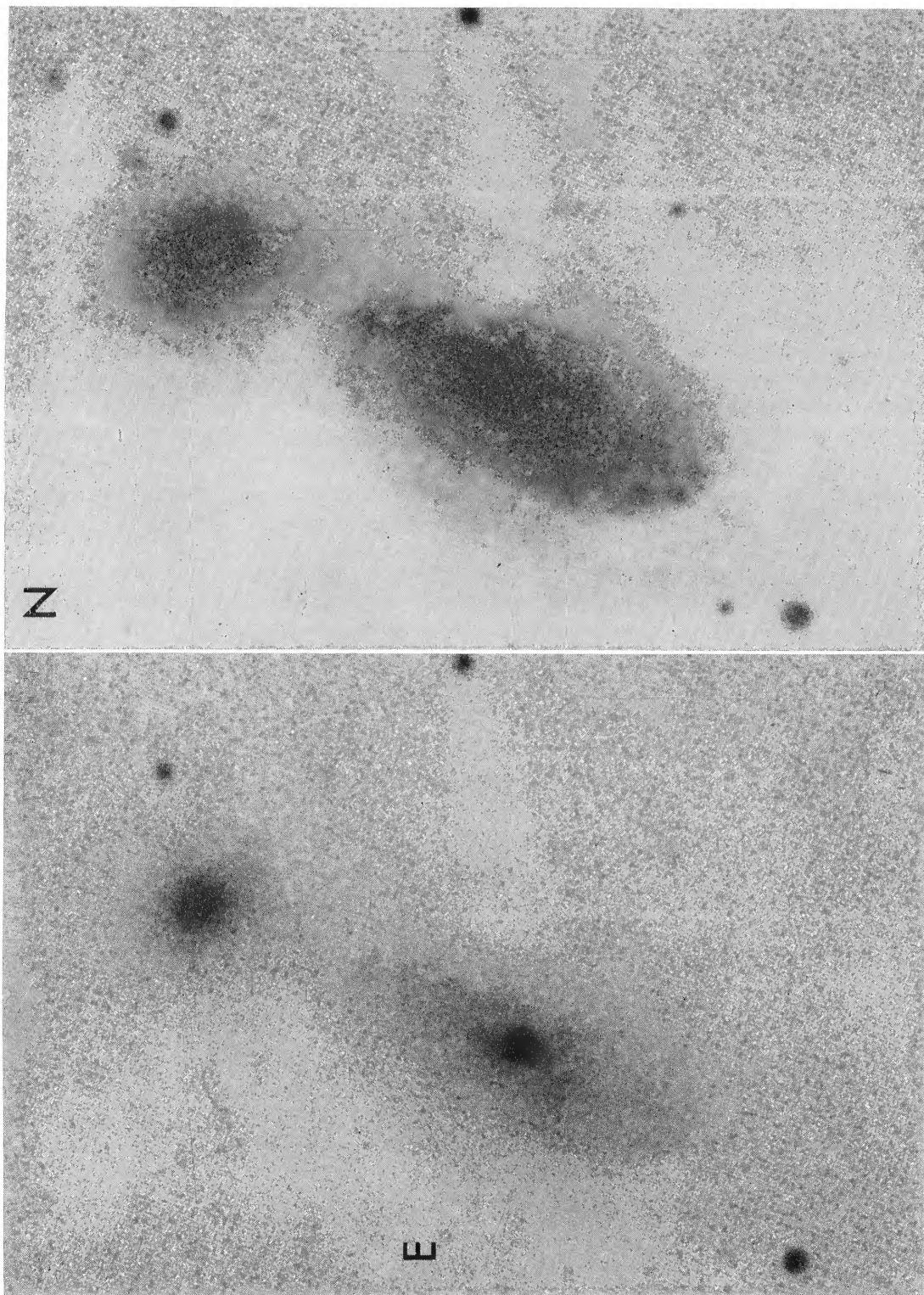


FIG. 1.—NGC 3227 and NGC 3226. *Left*: 116-min exposure, 40-inch reflector, U.S. Naval Observatory, 103aO emulsion + GG13 filter, which shows the structure near the nucleus. *Right*: Palomar Sky Survey print, 103aO emulsion, copyright 1957, National Geographic Society—Palomar Observatory Sky Survey. A faint, outer ringlike structure is off the field of this copy. For both prints, 1 mm = 2".75.

RUBIN AND FORD (see page 431)

versities at Lowell Observatory and the 84-inch Kitt Peak telescope. These spectra were obtained with the aid of an RCA C33011 cascaded image tube that was made available by the Carnegie Image Tube Committee. The tube has an S20 photosurface. The spectra are centered at 5800 Å and extend roughly from 4100 to 7300 Å. A record of observations is contained in Table 1. The plates with a dispersion of 270 Å mm⁻¹ were taken at Lowell Observatory; the scale perpendicular to the dispersion is 42'' mm⁻¹. Most plates with a dispersion of 132 Å mm⁻¹ were taken at Kitt Peak; the scale perpendicular to the dispersion is 35'' mm⁻¹. At this dispersion the nightsky sodium D-lines are just resolved, which indicates a limiting resolution on the plates of about 45 μ. This corresponds to a resolution of 1".6 perpendicular to the dispersion. Guiding is done on an offset star, with the galaxy held fixed on the slit, to maintain this spatial resolution.

In the nucleus of NGC 3227 we observe emission lines of [O III] λ4363, Hβ, [O III] λλ4959, 5007, [N I] λ5198, [O I] λλ6300, 6364, [N II] λ6548, Hα, [N II] λ6583, [S II]

TABLE 1
RECORD OF OBSERVATIONS

| Plate | Object (NGC) | Date (U.T.) | Exposure (min) | Dispersion (Å mm ⁻¹) | Position Angle of Slit (degrees) | Remarks |
|---------|--------------|-------------------|----------------|----------------------------------|----------------------------------|-----------------------------------|
| 1260a*† | 3227 | March 7, 1967 | 6 | 132 | 158 | Major axis, nucleus centered |
| 1260b*† | 3227 | March 7, 1967 | 31 | 132 | 158 | Major axis, nucleus centered |
| 1268a*† | 3227 | March 8, 1967 | 5 | 132 | 68 | Minor axis, nucleus centered |
| 1268b*† | 3227 | March 8, 1967 | 32 | 132 | 68 | Minor axis, nucleus centered |
| 1274*† | 3227 | March 8, 1967 | 120 | 132 | 158 | Major axis, nucleus centered |
| 1399† | 3227 | January 5, 1968 | 108 | 132 | 90 | Widened |
| 1180* | 3226 | December 14, 1966 | 120 | 270 | 7 | Nucleus and outer arm of NGC 3227 |
| 1185 | 3226 | December 15, 1966 | 60 | 270 | 34 | Major axis, nucleus |
| 1189 | 3226 | December 16, 1966 | 104 | 270 | 34 | Major axis, nucleus |
| 1276*† | 3226 | March 10, 1967 | 68 | 132 | 34 | Major axis, nucleus |
| 1398 | 3226 | January 5, 1968 | 75 | 132 | 90 | Widened |
| 1410 | 3226 | January 6, 1968 | 105 | 132 | 7 | Nucleus and outer arm of NGC 3227 |

* Measured for velocity

† Traced for line intensities.

λλ6717, 6731, and [O II] λ7330. Hγ is present but blended with the Hg λ4358 nightsky line. He I λ5875 is probably present in emission but not measurable because its redshift causes it to blend with the terrestrial sodium D-lines. He II λ4686 is not observed. We also observe, in second order, the blended [O II] λλ3727, 3729 doublet and [Ne III] λ3869. All of these lines are seen in spectra of other Seyfert galaxies. In the absorption-line spectrum, the sodium D-lines are most prominent, but additional features are also seen: λ4174, Ca I λ4227, the G-band, Mg I λ5176, and unidentified blends at λλ5800 and 6270. In the second-order spectrum, strong absorption is seen at λλ3774, 3804, and 3838. These latter two features are due to iron and magnesium and are observed in stars of type G (McCarthy and Rubin 1963); the λ4174 blend of Fe II and Ti II is used as a luminosity discriminant by Nassau and van Albada (1947).

The appearance on the plates of the emission lines in the nucleus is strongly dependent upon exposure time. On plates of shortest exposure, Hα is broad but broken into separate emission components, Hβ is so broken as to be hardly visible against the background continuum, while the [O III] lines are always compact and sharply defined. On longer exposures, the increase in density of Hα causes it to appear as a single line. Finally,

on longest exposures, the [N II] $\lambda\lambda 6548, 6583$ and H α configuration blends into one band about 6000 km sec^{-1} broad. Intensity profiles, discussed in detail below, show that wings of H α of almost this width are present even on plates of shortest duration. The effective angular extent of the region giving rise to the nuclear emission increases with exposure time; for moderate exposures a value of $3''\text{--}4''$ is typical. It is this region which we call the nucleus.

Spectroscopically, there is a sharply defined nucleus with a moderately intense continuum. At the boundary of the nuclear emission, discrete blobs of H α emission are observed. The most noticeable one is blueward of the sharp H α emission line on the north-west edge of the nucleus, giving the line a very asymmetrical appearance. In the disk, sharp lines of H α and [N II] are observed with almost no continuous spectrum. This can be seen in Figure 2 (Plate 3), where we show three spectra along the major axis of NGC 3227; exposures are 6, 31, and 120 min. On the longest exposure, emission lines can be observed outside the nucleus but bordering it and also arising from an emission region $70''$ from the nucleus.

The spectrum of the elliptical companion NGC 3226 has a strong continuum with many absorption features, of which the sodium D-lines and the Mg I triplet are strongest in this spectral region. Emission lines of H α , [N II] $\lambda\lambda 6548, 6583$, and H β are present. Plate 1180, taken with the slit of the spectrograph placed along the nucleus of NGC 3226 and the outer arm of NGC 3227, shows sharp H α emission in the region $35''\text{--}53''$ from the nucleus of NGC 3226, corresponding to the location of the connecting arm.

III. THE VELOCITY FIELD

During the several years that we were gathering spectra of NGC 3227 and NGC 3226, the quality of the spectra improved markedly, due principally to the recent use of a new Cassegrain-Schmidt spectrograph camera designed by Bowen. The velocity measurements are therefore based on these latter plates. The plates were measured on a Mann two-dimensional measuring machine. Each plate was measured twice, with the plate rotated 180° between measures. The cross-wires are set at 45° to the direction of travel, so that each measure is independent of other positions of the line. The reduction is carried out on an IBM 1130 and follows closely that used by Burbidge, Burbidge, and Prendergast (1959). The distortions due to the Schmidt camera-image tube system are corrected for in the reduction procedure, which is described elsewhere (Ford and Rubin 1967). The curvature across each line is a function of wavelength; it amounts to -2μ at the center of lines near 5000 \AA , and increases to $+6 \mu$ for lines near 6600 \AA . At this dispersion, $1 \mu = 6 \text{ km sec}^{-1}$.

As a check on the reduction procedure, the night sky line [O I] $\lambda 6300$ is measured across the spectrum. This line is near H α on the plate and is generally of comparable intensity. For two plates of NGC 3227 with widely different exposure times, measures of the night sky line are given in Table 2. From these results, we draw several conclusions. First, the reduction procedure has adequately taken account of the distortions, for the residuals along the night sky line are not systematic. Second, the mean observed wavelength differs by a few tenths of an Ångstrom from the laboratory wavelength. This will not affect relative measures across a single plate used for determining rotation curves. Finally, the accuracy of a single measurement, *for a sharp emission line*, is of the order of 10 km sec^{-1} . For broad, indistinct features such as those in a Seyfert galaxy, the accuracy must be considerably less.

In Table 3 we list the measured velocities from six plates, as a function of distance from the centers of NGC 3227 and NGC 3226. The position angle of the major axis of NGC 3227 is measured as 158° ; for NGC 3226 it is 34° . In Figure 3 are plotted the measured velocities from all plates taken with the slit along the major axis. In the nuclear region of strong continuum, $-3'' \leq y \leq +3''$, there is a large scatter in the measured velocities, but we attribute it to the difficulty of measuring broad, diffuse lines on plates

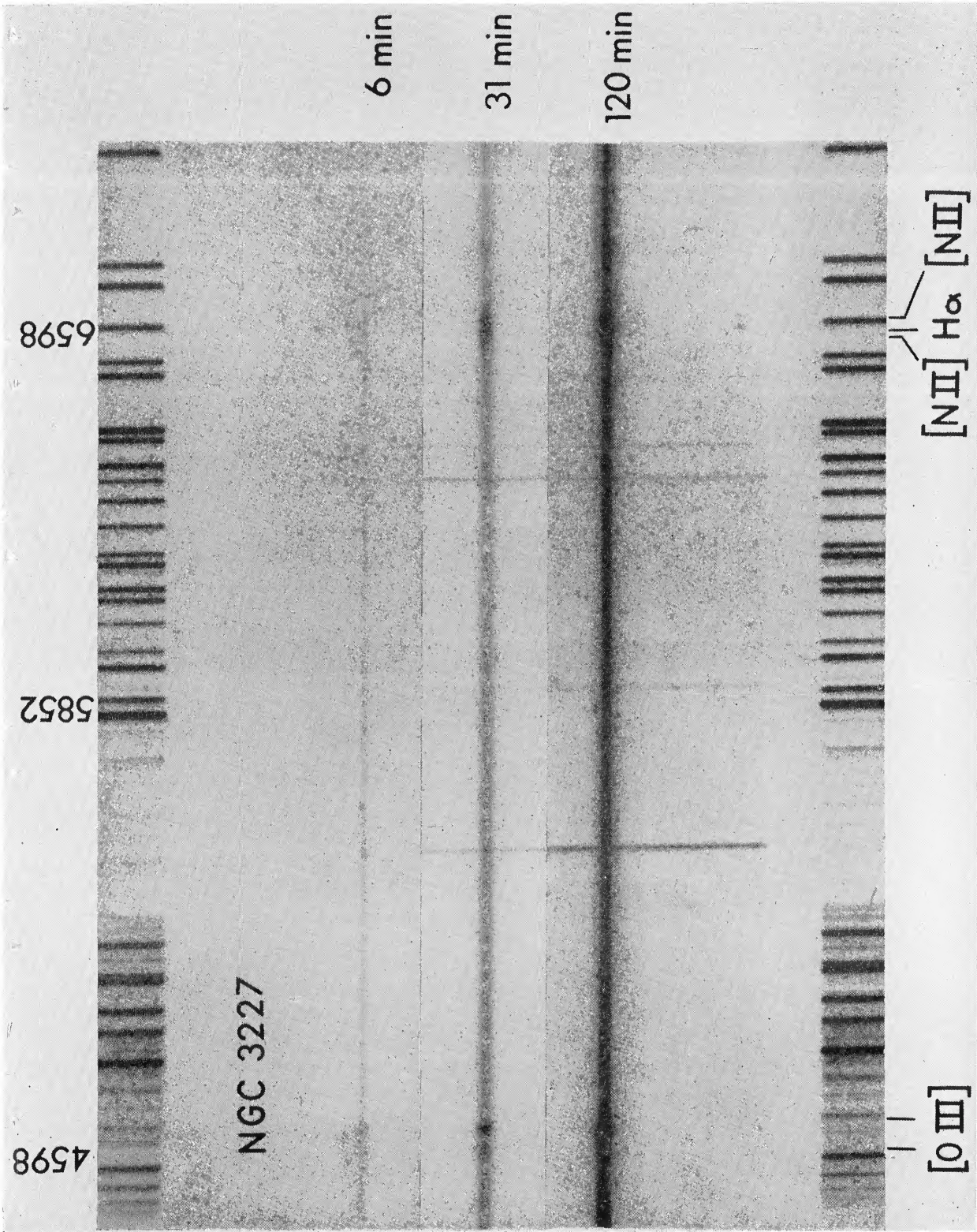


FIG. 2.—Three spectra taken with the slit along the major axis of NGC 3227. Original dispersion 132 \AA mm^{-1} ; neon and iron comparison spectrum. The [O III] $\lambda\lambda 4959, 5007$, [N II] $\lambda\lambda 6548, 6583$, and H α lines are indicated. On the 120-min exposure, H α and [N II] $\lambda 6583$, originating in the $70''$ emission region, may be seen near the lower edge of the print.
 RUBIN AND FORD (see page 433)

TABLE 2
MEASURES OF THE NIGHTSKY [O I] λ 6300.23 LINE

| PLATE 1260b | | | PLATE 1274 | | |
|--------------------------|-------------------------------------|---|--------------------------|-------------------------------------|--|
| Distance along Slit (mm) | $\lambda(\text{obs})$ (Å) | $\lambda - \langle \lambda \rangle$ (Å) | Distance along Slit (mm) | $\lambda(\text{obs})$ (Å) | $\lambda - \langle \lambda \rangle$ (Å) |
| -1 7 | 6299 93 | -0 22 | -1 9 | 6299 98 | +0 02 |
| -1 4 | 6299 93 | - 22 | -1 7 | 6299 75 | - 21 |
| -1 1 | 6300 17 | + 02 | -1 5 | 6300 12 | + 16 |
| -0 8 | 6300 64 | + 49 | -1 3 | 6300 00 | + 04 |
| -0 5 | 6300 33 | + 18 | -1 1 | 6300 03 | + 07 |
| -0 2 | 6300 32 | + 17 | -0 9 | 6300 02 | + 06 |
| +0 1 | 6299 90 | - 25 | -0 7 | 6299 97 | + 01 |
| +0 4 | 6299 91 | - 24 | -0 5 | 6300 02 | + 06 |
| +0 7 | 6300 00 | - 14 | -0 3 | 6299 86 | - 10 |
| +1 0 | 6299 99 | - 16 | -0 1 | 6300 34 | + 38 |
| +1 3 | 6299 84 | - 31 | +0 1 | 6300 43 | + 47 |
| +1 6 | 6300 12 | - 03 | +0 3 | 6299 98 | + 02 |
| +1 9 | 6300 19 | + 04 | +0 5 | 6299 75 | - 21 |
| +2 1 | 6300 84 | +0 69 | +0 7 | 6299 80 | - 16 |
| | | | +0 9 | 6300 03 | + 07 |
| | | | +1 1 | 6300 05 | + 09 |
| | | | +1 3 | 6299 78 | - 18 |
| | | | +1 5 | 6300 15 | + 19 |
| | | | +1 7 | 6300 15 | + 19 |
| | | | +1 9 | 6300 20 | + 24 |
| | | | +2 1 | 6299 11 | - 85 |
| | | | +2 3 | 6299 74 | -0 22 |
| | $\langle \lambda \rangle = 6300 15$ | $\langle \lambda - \langle \lambda \rangle \rangle$ = 0 22 Å = 1 7 μ = 10 8 km sec ⁻¹ | | $\langle \lambda \rangle = 6299 96$ | $\langle \lambda - \langle \lambda \rangle \rangle$ = 0 18 Å = 1 3 μ = 8 6 km sec ⁻¹ |

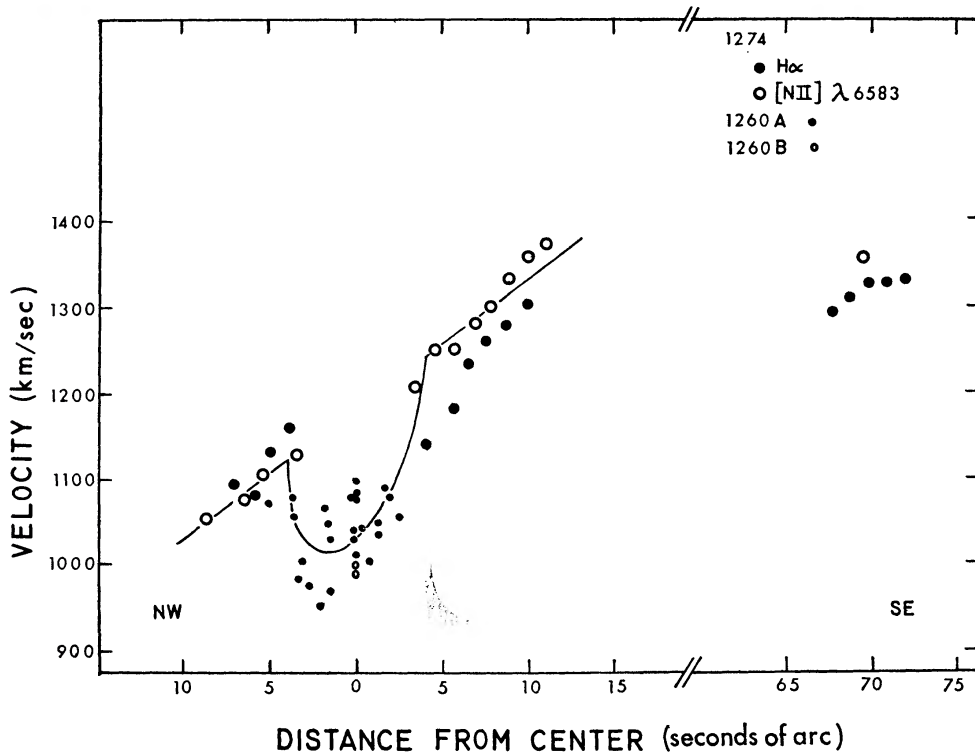


FIG. 3.—Observed velocities along major axes of NGC 3227. Observations in nucleus extend from $-4''$ to $+3''$. The line is drawn for a simple model in which expansion motions in the nucleus are superimposed upon rotation in the disk. Velocities at $70''$ and $75''$ come from...
American Astronomical Society. Provided by the NASA Astrophysics Data System

of different exposure times with different intensities of the continuous spectrum. In general, the $H\alpha$ measures give high velocities and the [O III] lines give low velocities, but the nearby [N II] $\lambda 6583$ line is probably responsible for the high $H\alpha$ measures. As a check on the line-to-line scatter on a single plate, eight lines were measured in the spectrum of NGC 4038, a galaxy with sharp lines in its spectrum. The velocities from individual lines showed significantly less scatter than the measures in NGC 3227. While it is possible that real differences in velocities do exist between the regions emitting $H\alpha$ and those giving rise to the forbidden lines, higher dispersion is necessary to establish such velocity variations. Hence we conclude that the line-to-line scatter in velocities in the nucleus is more probably due to observational effects.

The spectrum of the disk surrounding the nucleus has no continuum, and the emission lines are very sharp. However, there is a striking difference of about 150 km sec^{-1} between the velocities observed in the nucleus and those observed in the disk. It is not possible to measure velocities from both regions on a single plate because of the vast difference in intensity. However, the satisfactory agreement of the night-sky measures

TABLE 3
MEASURED VELOCITIES IN NGC 3227 AND NGC 3226

| Line | Y^* (arc sec) | V (km sec^{-1}) | Line | Y^* (arc sec) | V (km sec^{-1}) |
|---------------------------------|--------------------|---------------------------------|--------------------------------|--------------------|---------------------------------|
| NGC 3227 | | | NGC 3227 | | |
| Plate 1260a, P.A. 158° : | | | Plate 1274, P.A. 158° : | | |
| [O III] $\lambda 4959$ | 0 | 987 | $H\alpha$ | - 7 2 | 1093 |
| [O III] $\lambda 5007$ | 0 | 997 | | - 6 0 | 1082 |
| Plate 1260b, P.A. 158° : | | | | - 4 6 | 1131 |
| $H\beta$ $\lambda 4861$ | -2 2 | 953 | | - 3 6 | 1160 |
| | +0 8 | 1007 | | + 4 4 | 1138 |
| [O III] $\lambda 4959$ | -2 7 | 987 | | + 5 6 | 1180 |
| | -1 4 | 1032 | | + 6 6 | 1234 |
| | 0 | 1034 | | + 7 6 | 1258 |
| | +1 4 | 1042 | | + 8 6 | 1280 |
| [O III] $\lambda 5007$ | -4 1 | 937 | | + 9 8 | 1310 |
| | -2 9 | 982 | | +67 6 | 1294 |
| | -1 4 | 969 | | +68 6 | 1310 |
| | 0 | 1042 | | +69 6 | 1326 |
| | +1 3 | 1040 | | +70 7 | 1328 |
| | +2 7 | 1052 | | +71 8 | 1334 |
| Na $\lambda 5892$ | 0 | 1015 | [N II] $\lambda 6583$ | - 8 8 | 1053 |
| [O I] $\lambda 6300$ | 0 | 1082 | | - 7 7 | 1064 |
| $H\alpha$ | -5 2 | 1071 | | - 6 6 | 1074 |
| | -3 5 | 1080 | | - 5 6 | 1103 |
| | -1 7 | 1069 | | - 4 6 | 1112 |
| | 0 | 1079 | | - 3 5 | 1129 |
| | +1 7 | 1090 | | + 3 6 | 1206 |
| [N II] $\lambda 6583$ | -4 9 | 971 | | + 4 6 | 1248 |
| | -3 1 | 1008 | | + 5 7 | 1249 |
| | -1 7 | 1051 | | + 6 8 | 1276 |
| | +0 3 | 1045 | | + 7 8 | 1299 |
| | +1 9 | 1081 | | + 8 8 | 1335 |
| [S II] $\lambda 6717$ | 0 | 1098 | | + 9 9 | 1362 |
| [S II] $\lambda 6731$ | 0 | 1076 | | +11 0 | 1376 |
| | | | | +69 2 | 1365 |

* For position angle 158° , northwest identified by minus sign, southeast identified by plus sign; for position angles 68° , 34° , and 7° , southwest identified by minus sign, northeast by plus sign.

TABLE 3—Continued

| Line | Y^* (arc sec) | V (km sec ⁻¹) | Line | Y^* (arc sec) | V (km sec ⁻¹) |
|--|--------------------|--------------------------------|--|--------------------|--------------------------------|
| NGC 3227 | | | NGC 3227 | | |
| Plate 1268a, P.A. 68°: [O III] λ 5007 | -2 1 | 962 | Plate 1268b, P.A. 68°: [O III] λ 4959 | 0 | 1008 |
| | -1 1 | 965 | [O III] λ 5007 | 0 | 976 |
| | 0 | 958 | Na λ 5892 | 0 | 1039 |
| | +1 0 | 993 | NGC 3226 | | |
| | +2 1 | 974 | Plate 1276, P.A. 34°: Na λ 5892 | 0 | 1374 |
| H α em. | -2 1 | 820 | H α | 0 | 1344 |
| | -1 0 | 824 | [N II] λ 6583 | 0 | 1330 |
| | 0 | 842 | Outer Arm of NGC 3227 | | |
| | +1 0 | 850 | Plate 1180, P.A. 7°: H α | +34 9† | 591 |
| | +2 1 | 860 | | 36 5 | 556 |
| | +3 2 | 862 | | 38 2 | 608 |
| | +4 2 | 834 | | 39 9 | 602 |
| H α abs. | -2 1 | 966 | | 41 6 | 619 |
| | -1 1 | 972 | | 43 3 | 625 |
| | 0 | 958 | | 45 0 | 612 |
| | +1 1 | 973 | | 46 6 | 600 |
| H α em. | -2 1 | 1106 | | 48 3 | 539 |
| | -1 1 | 1088 | | 50 0 | 472 |
| | 0 | 1097 | | 51 7 | 538 |
| | +1 0 | 1108 | | +53 3 | 417 |
| | +2 1 | 1112 | | | |
| [N II] λ 6583 | -2 1 | 979 | | | |
| | -1 0 | 986 | | | |
| | 0 | 950 | | | |
| | +1 0 | 952 | | | |
| | +2 1 | 967 | | | |
| | +3 1 | 985 | | | |
| | +4 1 | 977 | | | |

† Seconds of arc from NGC 3226

for plates 1260b and 1274 (Table 2), the plates which give rise to the nucleus-disk velocity difference, gives us confidence that this difference is real; it is not likely that plate-to-plate differences of 150 km sec⁻¹ exist. Possible interpretations of this velocity difference will be discussed below.

In Figure 4 we plot the measured velocities along the minor axis of NGC 3227. On the plate of shortest exposure, several components are observed for H α , and velocities have been measured for two of these: one component, with a velocity near 1100 km sec⁻¹, and a blueward component, with a velocity of 840 km sec⁻¹. These distinct components show on the intensity profile of the line (Fig. 6). However, the sandwiching of H α between the two [N II] lines makes it impossible to resolve many of the separate velocity features at this dispersion. It would be valuable to observe the nucleus of NGC 3227 at higher dispersion, as Walker (1968) has done for NGC 1068, to examine the multiple velocity components which are present. However, the observational difficulties are increased, because the nucleus of NGC 3227, with a magnitude $V = 14.3$ (Dibay and Pronik 1967), is fainter than that of NGC 1068, for which $V = 13.0$ (Seyfert 1943).

For the lines [O III] λ 5007, 4959, Na λ 5892, [N II] λ 6583, velocities near 975 km sec⁻¹ are measured in the nucleus, for the plates taken along the minor axis. These

values agree moderately well with the low velocities measured for the nucleus, with plates along the major axis (Fig. 3).

There is no straightforward interpretation of the observed variation of velocity with position along the major axis of NGC 3227 (Fig. 3). From velocities in the nucleus (Figs. 3 and 4), a central velocity of about 1000 km sec^{-1} is observed for both emission and absorption lines. However, if this velocity is adopted as the systemic velocity of the galaxy, then all velocities in the disk are redshifted with respect to the nucleus, with a curious linear relation between disk velocity and distance in the galaxy. It is difficult to see how such a velocity field could exist for long without distorting the appearance of the galaxy.

Rather than adopt such a model, we prefer to assume that the linear portion of the rotation curve arises from a rotating spheroidal mass and that embedded in this mass are gas clouds expanding from the nucleus with a component of velocity in the line

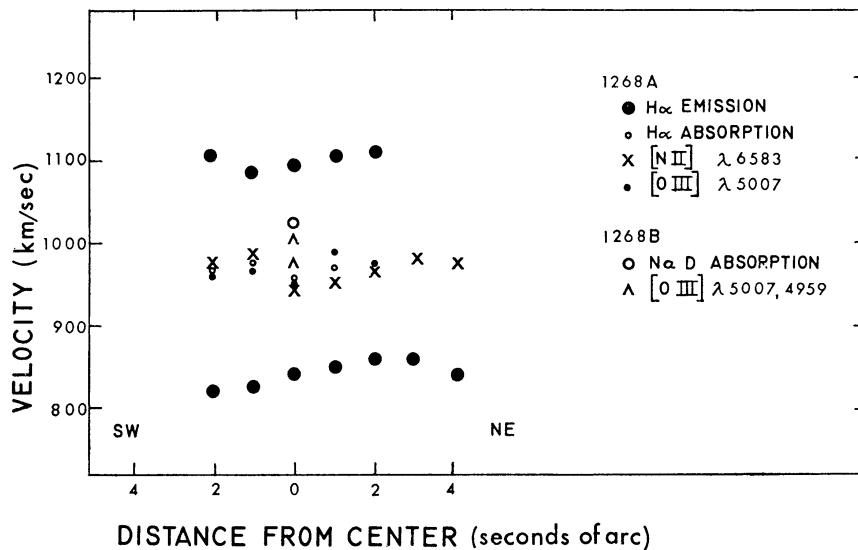


FIG. 4.—Observed velocities along the minor axis of NGC 3227

of sight. We also postulate the presence of dust and obscuring matter in the nucleus, so that we observe only clouds on the nearer side of the galaxy. This would require that the sodium D absorption lines in the nucleus arise in the gas clouds rather than in stars. There is growing evidence that a significant part of the sodium D absorption lines in spectra of galaxies arises in the gas, from synthesized spectra of M31 (Spinrad 1967), and from spectra of NGC 1808 (Burbidge and Burbidge 1968). It is also interesting to recall that Seyfert (1954) noted the abnormally broad ($>4000 \text{ km sec}^{-1}$) K-line in the Seyfert galaxy NGC 7469, and wrote, "It is extremely unlikely that the stars in the nucleus are moving with these tremendous velocities." Hence we prefer to determine the systemic velocity of NGC 3227 by extrapolating the disk velocities across $Y = 0$, and we obtain $V_{\text{sys}} = 1175 \text{ km sec}^{-1}$.

For a model with expansion velocities in the nucleus superimposed upon rotational velocities in the disk, the resulting rotation curve is shown by the solid line in Figure 3. A velocity of expansion of 175 km sec^{-1} has been assumed in the plane of NGC 3227.

We wish to emphasize that the measured velocities in the nucleus come from short-exposure observations of the nucleus. It is interesting to recall that from observations only of the disk of the Seyfert galaxy NGC 1068, Burbidge *et al.* (1959) inferred just such an effect in the velocity field of that galaxy. The observed velocities in the disk, ex-

trapolated across the nucleus of the galaxy, gave a central velocity several hundred kilometers per second higher than the central velocity determined from earlier studies (presumably from H and K absorption lines). They assumed that this was due to an expansion in the nucleus of NGC 1068 and that a real velocity difference existed between the gas giving rise to the sharp-lined (disk) and the broad-lined (nuclear) emissions. However, they had no actual measures across the nucleus. Similarly, the observations of NGC 1068 of Walker (1968) are generally long exposures to study the outer regions. Hence, conclusions concerning motions of the discrete clouds, which he observes bordering the nucleus, are obtained by extrapolating through the nucleus. However, his figures showing the extension of the broad emissions above and below the nucleus indicate that the average velocity of all the broad components differs from the mean velocity of the sharp emission by -230 km sec^{-1} . In contrast to this, our evidence for an expansion in the nucleus of NGC 3227 comes from direct measures.

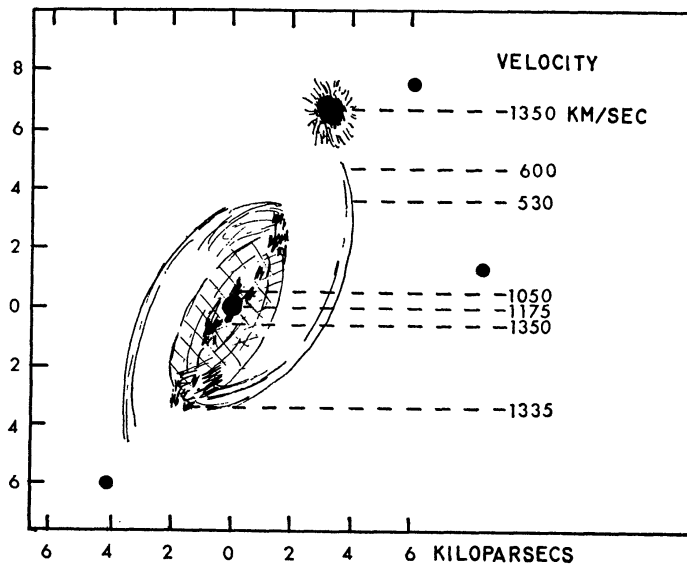


FIG. 5.—Sketch of NGC 3226/3227 indicating observed velocities

We adopt a velocity of 1175 km sec^{-1} for the systemic velocity of NGC 3227; $V = 1349 \text{ km sec}^{-1}$ for the velocity of NGC 3226. These correspond to velocities of $V = 1069 \text{ km sec}^{-1}$ and $V = 1243 \text{ km sec}^{-1}$, corrected for a rotation of the Sun of 300 km sec^{-1} about the center of our Galaxy. Earlier velocities for these galaxies are $V = 1111 \text{ km sec}^{-1}$ and $V = 1338 \text{ km sec}^{-1}$ (uncorrected) from Humason, Mayall, and Sandage (1956). If we choose the average velocity obtained here as the systemic velocity of the system, $V_{\text{sys}} = 1156 \text{ km sec}^{-1}$. For a Hubble constant of $100 \text{ km sec}^{-1} \text{ kpc}^{-1}$, this corresponds to a distance of $1.2 \times 10^7 \text{ pc}$. At this distance, $1'' = 56 \text{ pc}$; the radius of the nucleus is about 200 pc , and the projected separation between NGC 3227 and NGC 3226 is 7300 pc . Velocities in the disk are observed to a distance of 620 pc ; there are additional measures at 3900 pc . If we assume that the connecting arm between NGC 3227 and NGC 3226 is coplanar with NGC 3227, it is located at a mean distance of 5600 pc from the nucleus of NGC 3227. The observed mean velocity of the arm, $V = 550 \text{ km sec}^{-1}$, is 700 km sec^{-1} less than the systemic NGC 3226/3227 velocity. A sketch of NGC 3226/3227 is shown in Figure 5 with the observed velocities indicated. For the interconnected galaxies studied by Zwicky and Humason (1960, 1961), no velocity differences as large as this are reported.

It is of interest to examine briefly the stability of the NGC 3226/3227 system. From the distribution of galaxies over the sky, Page (1961) has shown that the chances are better than 90 per cent that a given pair is physically related. In the case of NGC 3226/3227, the connecting arm makes the association unquestionable. The magnitude of NGC 3226 is $m = 12.7$ (de Vaucouleurs and de Vaucouleurs 1964); if we adopt a mass/luminosity (\mathcal{M}/L) ratio 20 times as great for elliptical galaxies as for spiral galaxies, then $\mathcal{M}_{3226} = 3.0 \times 10^{11} \mathcal{M}_{\odot}$; $\mathcal{M}_{3227} = 3 \times 10^{10} \mathcal{M}_{\odot}$, from the value determined below. For a circular orbit, the orbital velocity of NGC 3227 must be over 450 km sec^{-1} with respect to NGC 3226, and the period greater than 10^8 years. The observed velocity in the line of sight is 170 km sec^{-1} ; for stability, the transverse components must be larger than this value. If each transverse component just equals the observed radial component, NGC 3227 will fall into NGC 3226 in a time $T = 4 \times 10^7$ years.

The stability of the connecting arm is a puzzle. If NGC 3226 lies in the plane of the disk of NGC 3227, then the region of the arm we have observed actually lies several thousand parsecs closer to NGC 3226 than to NGC 3227. (The only evidence that NGC 3226 and NGC 3227 are coplanar is the fact that the position angle of the line joining them is 167° , close to the position angle of the major axis of NGC 3227. It could, of course, actually be at a much greater distance.) NGC 3226, with the greater mass, must produce a significant perturbing effect on the arm. Yet the very regular look of the arm gives no evidence of such an effect.

IV. MASS OF NGC 3227

With the exception of the few velocities observed at $r = 3900 \text{ pc}$, the velocity curve extends only to $r = 620 \text{ pc}$ from the center of NGC 3227. We will first determine the mass out to this distance. We assume a model with the mass distributed over a single uniform spheroid; this mass distribution gives rise to a linear rotation curve. From the equations given by Burbidge *et al.* (1959), adopting the ratio of minor axis to major axis $c/a = 0.2$, we obtain

$$\begin{aligned}\mathcal{M} &= 3.0 \times 10^9 \mathcal{M}_{\odot} \text{ to } r = 620 \text{ pc}, \\ \text{Density} &= 16 \mathcal{M}_{\odot} \text{ pc}^{-3} = 10^{-21} \text{ g cm}^{-3}, \\ V_{\text{escape}} &= 380 \text{ km sec}^{-1}.\end{aligned}$$

The velocity of escape from this inner region is sensitive to any uncertainty in the mass. For a more spherical nucleus with $c/a = 0.5$, $\mathcal{M} = 4.0 \times 10^9 \mathcal{M}_{\odot}$.

Corresponding values may be calculated from the velocities at 3900 pc , using a Keplerian approximation for the interior mass. The results are

$$\begin{aligned}\mathcal{M} &= 2.6 \times 10^{10} \mathcal{M}_{\odot} \text{ to } r = 3900 \text{ pc}, \\ \text{Density} &= 0.5 \mathcal{M}_{\odot} \text{ pc}^{-3} = 3 \times 10^{-23} \text{ g cm}^{-3}, \\ V_{\text{escape}} &= 440 \text{ km sec}^{-1}.\end{aligned}$$

It is interesting to compare these values with those for NGC 1068. We list some physical parameters in Table 4. The most notable feature of the comparison is that while the distances and masses of the two galaxies are similar, NGC 3227 is over 1 mag fainter, which results in a larger \mathcal{M}/L ratio for NGC 3227.

We know from the measured velocities that the mean cloud velocities in the nucleus are of the order of a few hundred kilometers per second with respect to the central velocity. This is less than the escape velocity. Thus, not all clouds are leaving the nucleus. Some may move out from the nucleus, interact with the interstellar medium, and end up rotating in bound orbits. But the $\text{H}\alpha$ profiles, to be discussed below, exhibit wings

several thousand kilometers per second in width. If this width is interpreted as a velocity broadening, then some clouds are escaping from the nucleus. Hence the lifetimes of the clouds must be of the order of 10^5 years, after which their velocities will carry them outside the nucleus.

Models for the nuclear regions of a Seyfert galaxy have recently been advanced by Dibay and Pronik (1967) and Oke and Sargent (1968). Although the models differ in detail, each postulates two physically distinct regions in the nucleus. This allows for the different physical parameters necessary for the production of emission lines of hydrogen, forbidden lines, and coronal lines (Oke and Sargent 1968). Both models require that energy for the mass motions of gas in the nucleus be continuously supplied. The radial velocities observed in the nucleus of NGC 3227 are consistent with these models.

TABLE 4
PHYSICAL PARAMETERS OF NGC 3227 AND NGC 1068

| Parameter | NGC 3227 | NGC 1068 |
|----------------------------|--|--|
| V (systemic) | 1156 km sec ⁻¹ (NGC 3227/3226) | 1125 km sec ⁻¹ (corrected for galactic rotation)* |
| Distance | 1.2×10^7 pc | 1.1×10^7 pc |
| Area on sky | $\begin{cases} 3.0 \times 1.2 \dagger \\ 3.7 \times 2.4 \ddagger \end{cases}$ | $\begin{cases} 2.5 \times 1.7 \dagger \\ 5.2 \times 4.4 \ddagger \end{cases}$ |
| Mass \mathcal{M} | $\begin{cases} 3 \times 10^9 \mathcal{M}_{\odot} \text{ to } r=620 \text{ pc} \\ 3 \times 10^{10} \mathcal{M}_{\odot} \text{ to } r=3900 \text{ pc} \end{cases}$ | $\begin{cases} 3 \times 10^9 \mathcal{M}_{\odot} \text{ to } r=2000 \text{ pc}^* \\ 3 \times 10^{10} \mathcal{M}_{\odot} \text{ to } r=2020 \text{ pc}^{\S} \end{cases}$ |
| Magnitude V (nucleus) | 14.3 \parallel | 13.0 $\#$ |
| Magnitude V (total) | 11.9 \ddagger | 10.3 \ddagger |
| M (nucleus) | -16.4 | -17.2 |
| M (total) | -18.8 | -19.9 |
| \mathcal{M}/L nucleus | 10 $\}$ | |
| \mathcal{M}/L to 3900 pc | 10 $\}$ | 2.1 to $r=2020$ pc \S |

* Walker (1968).

† Shapley and Ames (1932)

‡ De Vaucouleurs and de Vaucouleurs (1964).

§ Burbidge, Burbidge, and Prendergast (1959).

\parallel Dibay and Pronik (1967)

$\#$ Seyfert (1943).

V. LINE STRENGTHS IN NGC 3327 AND NGC 3326

The spectrum displayed by the final P11 phosphor of the image intensifier is photographed on baked IIaO plates. These plates are calibrated by exposing and developing a step-wedge plate simultaneously with the galaxy plate. The source of light for the calibrated step wedge is a P11 phosphor excited by a radioactive C¹⁴ source. The spectral response of the optical system has been calibrated by observing the nucleus of M31 and reducing the observed intensities to those obtained by Spinrad with a spectral scanner at the Lick 120-inch telescope and kindly supplied by him in advance of publication. Spinrad's M31 observations are in turn based on observations by Hayes (1967) of the standard stars 58 Aql and 29 Psc.

For NGC 3227 and NGC 3226, relative line strengths have been determined from seven plates. The individual measures, relative to H α , are listed in Table 5. They are corrected for extinction and the spectral response of the system but not for reddening. From the scatter for a single line it is estimated that the derived values are accurate to within 20 per cent, plus any additional error in the calibration of the spectral sensitivity of the system. For comparison, the line strengths for NGC 1068 from Osterbrock and Parker (1965) are listed. The major difference between the relative line strengths in the two galaxies is in the [O III] $\lambda\lambda 5007, 4959$ lines, which are relatively weaker in NGC 3227.

The [N II] $\lambda\lambda 6548, 6583$, and $H\alpha$ lines are not completely resolved, even on the shortest exposures, but intensities have been determined by making use of the known wavelength of each line and the known $\lambda 6548/\lambda 6583$ intensity ratio. We show in Figure 6 microphotometer tracings of the $H\alpha$ spectral region from plates 1268a, and 1268b, 5- and 32-min exposures, respectively. In Figure 7, the deduced intensity profiles are shown, along with the reconstruction of the $H\alpha$ and [N II] $\lambda\lambda 6548, 6583$ profiles and profiles of [O III] $\lambda\lambda 4959, 5007$. A tracing of plate 1260b, from $\lambda 4500$ to $\lambda 7000$, has been published elsewhere (Rubin and Ford 1967).

It is apparent from Figure 7 that the line profiles for the forbidden [O III] lines differ markedly from the profiles of the hydrogen lines. Both $H\alpha$ and $H\beta$ have a multicomponent structure which we believe arises from individual hydrogen clouds moving with different velocities and which is completely absent in the forbidden lines. Evidence of

TABLE 5
RELATIVE LINE STRENGTHS IN NGC 3227 AND NGC 3226

| LINE | NGC 3227 | | | | | | | | NGC 1068 (Osterbrock and Parker 1965) | NGC 3226 (Plate 1276) |
|------------------------|----------------|----------------|----------------|-----------------|-------------------------|------------------------|----------------|------|---|-----------------------------|
| | Plate 1260a | Plate 1260b | Plate 1268a | Plate 1268b* | Plate 1274 (Disk) | Plate 1274 (Arm) | Plate 1399† | Mean | | |
| [O III] $\lambda 4363$ | . | . | . | . | . | . | 0 23 | 0 23 | . | . |
| $H\beta$ | 0 62 | 0 48 | 0 60 | 0 57 | . | . | . | 0 57 | 0 8 | . |
| [O III] $\lambda 4959$ | 1 7 | 1 4 | 1 5 | .. | . | . | . | 1 5 | 4 5 | . |
| [O III] $\lambda 5007$ | 5 8 | 8 5 | 6 5 | .. | . | . | . | 6 9 | 13 | . |
| [N I] $\lambda 5198$ | . | 0 11 | . | 0 23 | . | . | . | 0 17 | 0 23 | . |
| [O I] $\lambda 6300$ | . | 0 39 | . | 0 42 | .. | . | 1 0 | 0 60 | 0 47 | . |
| [O I] $\lambda 6364$ | . | 0 13 | . | 0 12 | . | . | 0 23 | 0 16 | . | . |
| [N II] $\lambda 6548$ | 1 5 | 1 5 | 1 4 | . | 1 7 | 1 2 | . | 1 5 | 1 9 | 4 8 |
| $H\alpha$ core | 10 | 10 | 10 | . | 10 | 10 | . | 10 | 10 | 10 |
| $H\alpha$ core+wings | . | 13 | 14 | . | . | . | . | 14 | . | . |
| [N II] $\lambda 6583$ | 5 0 | 4 4 | 4 3 | . | 5 4 | 3 8 | . | 4 6 | 5 6 | 16 |
| [S II] $\lambda 6717$ | . | 1 4 | . | . | . | . | 1 4 | 1 4 | . | .. |
| [S II] $\lambda 6731$ | . | 1 0 | . | . | . | . | 1 0 | 1 0 | 1 7 | . |

* $H\beta$ set equal to 0 57.

† $\lambda 6731$ set equal to 1 0.

the multiple peaks of $H\alpha$ is present on plates of all exposure times, although not all peaks can be identified on each plate. This is seen in Figure 6. This multiplicity in the $H\alpha$ profile supports the view that the nucleus contains discrete hydrogen clouds, some moving with velocities of hundreds or thousands of kilometers per second with respect to the central velocity. To give some indication of the instrumental profile, we also show in Figure 7 two line profiles for the nightsky [O I] $\lambda 5577$ line: one from a short-exposure and one from a long-exposure plate.

To deduce conditions of temperature and density in the nucleus of NGC 3227 from the observed line intensities, we will assume that the reddening in our Galaxy and in the nucleus of NGC 3227 is small enough to neglect. (For NGC 3227, $b^r = 57^\circ$.) We will return to this assumption below. We realize that the line intensities are averages over large regions of space which must have wide ranges of temperatures and densities, as indicated by the wide ranges of ionizations and present in the emission-line spectrum.

Following Seaton (1960) and Osterbrock and Parker (1965), we use the [O III] ratio

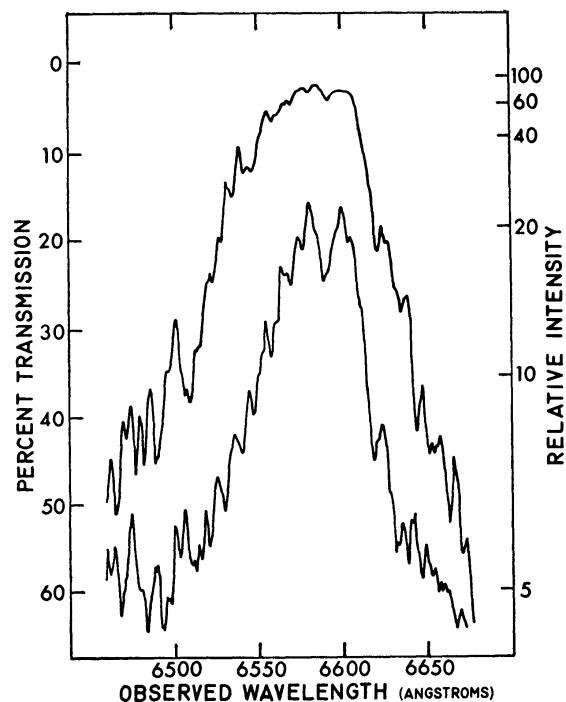


FIG. 6.—Microphotometer tracing of plate 1268a (5-min exposure) and plate 1268b (32-min exposure) near $H\alpha$.

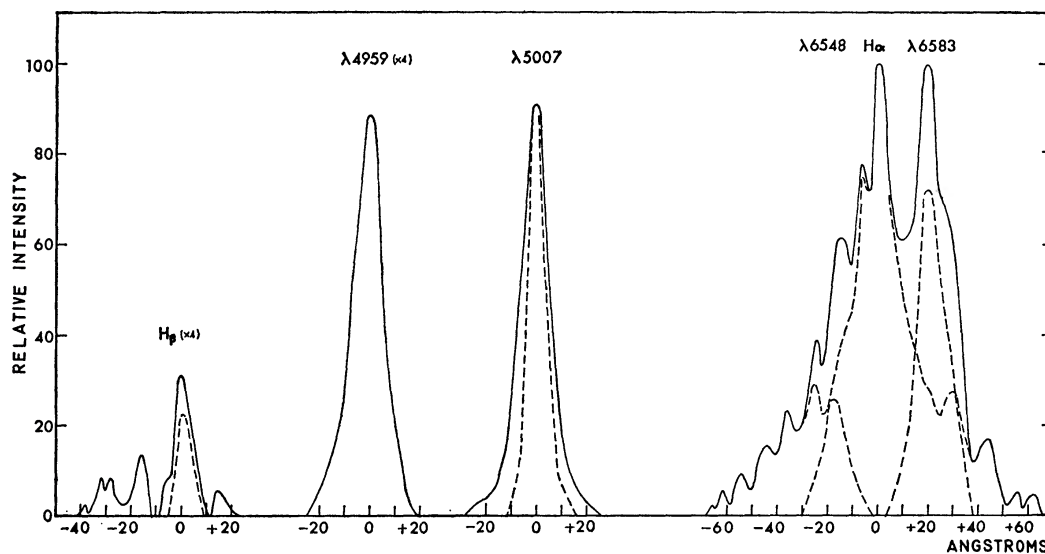


FIG. 7.—Line profiles from plate 1268a (5-min exposure) on relative-intensity scale. For the $H\alpha$ + $[N\ II]$ $\lambda\lambda 6548, 6583$ blend, the resolution into individual lines is indicated. Dotted line within $H\beta$ is the line profile for the nightsky $[O\ I]$ $\lambda 5577$ line, from plate 1268a. Dotted line within the $[O\ III]$ $\lambda 5007$ line is the $\lambda 5577$ profile from a longer-exposure (68-min) plate.

$I(\lambda 4959 + \lambda 5007)/I(\lambda 4363)$ to derive an electron temperature $T = 19000^\circ \text{K}$. This value is not well determined, because $[\text{O III}] \lambda 4363$ has been measured on one plate only; an error of ± 30 per cent in its intensity will produce an error of $\pm 5000^\circ$. Similarly, the $[\text{N II}]$ ratio $I(\lambda 6548 + \lambda 6583)/I(\lambda 5755)$ (unobserved) gives the upper limit $T < 11000^\circ$. This difference in temperature may reflect a real temperature difference in the regions where the $[\text{O III}]$ and the $[\text{N II}]$ lines arise, or it may merely reflect the uncertainties in the observations and calculations. For NGC 1068, using the same ratios as those used here, Osterbrock and Parker (1965) found values of $T = 10200^\circ$ and $T < 8200^\circ \text{K}$.

From the observed ratio of the $[\text{S II}]$ doublet, $r = I(\lambda 6717)/I(\lambda 6731)$, we can calculate the electron density N_e . Weedman (1968) has shown that this ratio can be used to deduce accurately N_e , except for values of the ratio near 1.50 and 0.38, which represent the low- and high-density limits, respectively. For NGC 3227, $r = 1.4$, so that the $[\text{S II}]$ lines must originate in a region of extreme low density. Using the expression for N_e from Weedman (1968), based on new collision strengths given by Czyzak *et al.* (1967), the calculated values for N_e range from 200 to 50 cm^{-3} for values of T between 10000° and 20000°K . Hence we conclude that the present observations indicate a slightly higher mean temperature and a lower mean density than corresponding values for NGC 1068. Whether this difference is significant, in view of the large regions that are being sampled, is open to question.

The observed intensity ratio $I(\text{H}\alpha)/I(\text{H}\beta) = 17$ is larger than the ratio of 3:1 predicted by recombination theory (Seaton 1960). While it is possible that the intensity of $\text{H}\beta$ is underestimated, because of the difficulty of establishing the continuum level for such a broken line, it is unlikely that the intensity could be increased by more than 50 per cent. For NGC 1068, Osterbrock and Parker (1965) attribute the observed high ratio (12.5:1) to self-absorption of the lines. This could be a factor in the observed intensities for NGC 3227 also. In addition, excessive reddening in the nucleus of NGC 3227 would also increase the $\text{H}\alpha/\text{H}\beta$ intensity ratio.

Finally, we may look at the ratio of $\text{H}\alpha$ to the $[\text{N II}]$ lines, $I(\text{H}\alpha)/I(\lambda 6548 + \lambda 6583)$. For emission regions in our Galaxy, this ratio is generally near 3 (Burbidge 1962 and references therein). In external galaxies, a value of 3:1 is common, although in the nuclei of some galaxies, the $[\text{N II}]$ lines are stronger than $\text{H}\alpha$. Such an effect is seen in the nucleus of M31 (Ford and Rubin 1968) and in NGC 3226. For the nucleus of NGC 3227, the intensity of the $\text{H}\alpha$ line is twice that of the $[\text{N II}]$ lines.

From the observed profiles, we can also determine line widths. For $\text{H}\alpha$ the maximum extent observed is 7200 km sec^{-1} , with 6000 km sec^{-1} about average in the nucleus. For $\text{H}\beta$ and $[\text{O III}] \lambda 5007$, widths of 3000 km sec^{-1} are typical in the nucleus. All other emission lines in the nucleus and all lines outside the nucleus have widths only slightly greater than the instrumental profile, which is about 900 km sec^{-1} as determined from the strong night sky $[\text{O I}] \lambda 5577$ profile. For the sodium D absorption line in the nucleus, the line width is about 1100 km sec^{-1} , or just broader than the instrumental profile.

Emission-line strengths in the spectrum of the elliptical galaxy NGC 3226 are listed in Table 5. They are of lower weight than the line strengths determined for NGC 3227, because of the difficulty introduced by the background continuum. $\text{H}\alpha$ and $[\text{N II}] \lambda 6583$ are each about 1000 km sec^{-1} broad. The sodium D absorption lines are 1500 km sec^{-1} wide and hence broader than those in NGC 3227. The intensity ratio $I(\text{H}\alpha)/I(\lambda 6548 + \lambda 6583) = 0.47$. The $\text{H}\alpha$ and $[\text{N II}] \lambda 6583$ lines are separated by a deep absorption feature measured at 6600 \AA , which gives a velocity $V = 1700 \text{ km sec}^{-1}$ if it is identified with $\text{H}\alpha$.

VI. CONCLUSIONS

We can summarize the results of this study by the following conclusions:

1. The nucleus ($r < 200 \text{ pc}$) of the Seyfert galaxy NGC 3227 shows emission lines in its spectrum, with the hydrogen lines resolved into multiple components. All lines show negative velocities with respect to the central velocity, $V = 1175 \text{ km sec}^{-1}$. A G-type

absorption spectrum is observed. The velocity of the sodium D-lines agrees with the velocities from the broad emission features and may be partly of interstellar (in NGC 3227) origin.

2. The nucleus of NGC 3227 is composed of discrete hydrogen clouds, some moving with velocities in excess of the escape velocity. The observed average negative velocity in the nucleus is produced by clouds expanding from the nucleus. The mean physical conditions of T and N_e within the emitting regions have been calculated.

3. The transition from the nucleus to the disk is abrupt, with some of the broad emission lines jutting out above the continuum from the nucleus. Sharp $H\alpha$ and $[N\ II]\ \lambda 6583$ lines are observed to $r = 600$ pc and exhibit a linear velocity curve. Emission is also observed in a region at $r = 3900$ pc.

4. Emission from the connecting arm between NGC 3227 ($V = 1175$ km sec $^{-1}$) and NGC 3226 ($V = 1349$ km sec $^{-1}$) shows a mean observed velocity of 550 km sec $^{-1}$, or a velocity of -700 km sec $^{-1}$ with respect to the mean NGC 3226/3227 velocity. If the arm lies in the plane of NGC 3227, it is 5600 pc from the nucleus, with a velocity in excess of the escape velocity. It is not clear whether the configuration is stable.

5. It may be significant that the high $H\alpha/H\beta$ ratio, the large mass/luminosity ratio, the similar velocities from the sodium D absorption lines and the broad emission lines, and the excess negative velocities in the nucleus all could be indicators that large amounts of absorbing material are present in the nucleus of the galaxy.

6. For the elliptical companion, NGC 3226, emission lines of $H\alpha$, $H\beta$, $[N\ II]\ \lambda\lambda 6548$ and 6583 are observed. The intensity ratio $I(H\alpha)/I(\lambda 6548 + \lambda 6583) = 0.47$.

From these observations, we can add NGC 3227 to that small list of Seyfert galaxies in which mass ejection from the nucleus is observed (NGC 1068, Walker 1968; NGC 1275, Burbidge and Burbidge 1965; NGC 4151, Oke and Sargent 1968). All the above conclusions support current ideas concerning the nuclei of Seyfert galaxies. Explosive phenomena must be taking place with time scales as short as 10^5 years, which accelerate discrete clouds to velocities in excess of the escape velocity. Masses of gas are leaving the nucleus; energies as high as 10^{55} ergs are involved. The work of Osterbrock and Parker (1965) shows that the source of ionization is most probably the kinetic energy in the collisions among the high-velocity clouds. The mechanism producing the required high velocities remains unexplained.

We wish to thank Dr. J. S. Hall, Director of the Lowell Observatory, Dr. N. U. Mayall, Director of the Kitt Peak National Observatory, and Dr. K. Aa. Strand, Scientific Director of the U.S. Naval Observatory, for making telescope time available. We also wish to thank Drs. E. M. and G. R. Burbidge for initial conversations about this galaxy, Rev. M. F. McCarthy, S.J., for assistance in obtaining some of the spectra, and Dr. K. Turner for his help with the study of the dynamics of the NGC 3227/3226 pair.

REFERENCES

- Burbidge, E. M. 1962, in *The Distribution and Motion of Interstellar Matter in Galaxies*, ed. L. Woltjer (New York: W. A. Benjamin, Inc.), p. 123.
 Burbidge, E. M., and Burbidge, G. R. 1965, *Ap. J.*, **142**, 1351.
 ———. 1968, *ibid.*, **151**, 99.
 Burbidge, E. M., Burbidge, G. R., and Prendergast, K. H. 1959, *Ap. J.*, **130**, 26.
 Burbidge, E. M., Burbidge, G. R., and Sandage, A. R. 1963, *Rev. Mod. Phys.*, **35**, 947.
 Czyzak, S. J., Krueger, T. K., Martins, P. de A. P., Saraph, H. E., Seaton, M. J., and Shemming, J. 1967, I.A.U. Symposium on Planetary Nebulae (to be published).
 Dibay, E. A., and Pronik, V. I. 1967, *Astr. Zh.*, **44**, 952.
 Ford, W. K., Jr., and Rubin, V. C. 1967, *Carnegie Yrb.*, **66**, 137.
 ———. 1968, *ibid.*, Vol. 67 (in press).
 Hayes, S., 1967 (unpublished).
 Humason, M. L., Mayall, N. U., and Sandage, A. R. 1956, *A. J.*, **61**, 97.
 McCarthy, M. F., S. J., and Rubin, V. C. 1963, *Spec. Astr. Vaticana*, **6**, 432.

- Morgan, W. W. 1959, *Pub. A.S.P.*, **71**, 394
 Nassau, J. J., and Albada, G. B. van 1947, *Ap. J.*, **106**, 20.
 Oke, J. B., and Sargent, W. L. W. 1968, *Ap. J.*, **151**, 807.
 Osterbrock, D. E., and Parker, R. A. R. 1965, *Ap. J.*, **141**, 892.
 Page, T. 1961, in *Proceedings of the Fourth Berkeley Symposium*, Vol. 3, ed J. Neyman (Berkeley and Los Angeles: University of California Press), p. 277.
 Rubin, V. C., and Ford, W. K., Jr. 1967, *Pub. A.S.P.*, **79**, 322.
 Seaton, M. J. 1960, *Rept. Progr. Phys.*, **23**, 313.
 Seyfert, C. K. 1943, *Ap. J.*, **97**, 28.
 ———. 1954, Berkeley Conference Lecture Notes (mimeograph), p. 221.
 Shapley, H., and Ames, A. 1932, *Harvard Ann.*, **88**, 43.
 Spinrad, H. 1967, invited discourse, I A U. meeting, Prague.
 Vaucouleurs, G. de, and Vaucouleurs, A. de. 1964, *Reference Catalogue of Bright Galaxies* (Austin: University of Texas Press).
 Walker, M. F. 1968, *Ap. J.*, **151**, 71.
 Weedman, D. W. 1968, *Pub. A.S.P.* (submitted)
 Zwicky, F., and Humason, M. L. 1960, *Ap. J.*, **132**, 627.
 ———. 1961, *ibid.*, **133**, 794.

Copyright 1968 The University of Chicago Printed in U.S.A.

1968AJ...154..431R